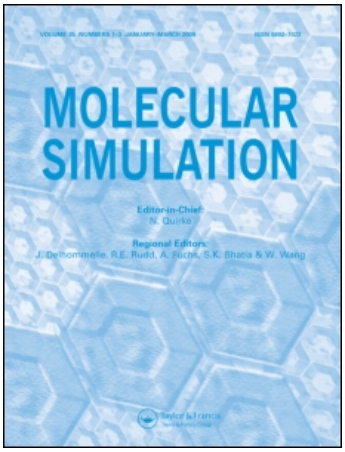

Molecular Simulation

Publication details, including instructions for authors and subscription information:
http://www.informaworld.com/smpp/title~content=t713644482

A molecular simulation approach to the study of adsorption of hydrogen cyanide and methyl ethyl ketone in silicalite, mordenite and zeolite beta structures

R. R. Kotdawala[a]; A. Ozgur Yazaydin[a]; N. Kazantzis[a]; R. W. Thompson[a]
[a] Department of Chemical Engineering, Worcester Polytechnic Institute, Worcester, MA, USA

To cite this Article Kotdawala, R. R. , Ozgur Yazaydin, A. , Kazantzis, N. and Thompson, R. W.(2007) 'A molecular simulation approach to the study of adsorption of hydrogen cyanide and methyl ethyl ketone in silicalite, mordenite and zeolite beta structures', Molecular Simulation, 33: 9, 843 — 850
To link to this Article: DOI: 10.1080/08927020701275068
URL: http://dx.doi.org/10.1080/08927020701275068

Molecular Simulation, Vol. 33, Nos. 9–10, 15–30 August 2007, 843–850

A molecular simulation approach to the study of adsorption of hydrogen cyanide and methyl ethyl ketone in silicalite, mordenite and zeolite beta structures

R. R. KOTDAWALA, A. OZGUR YAZAYDIN, N. KAZANTZIS and R. W. THOMPSON*

Department of Chemical Engineering, Worcester Polytechnic Institute, Worcester, MA 01609-2280, USA

(Received December 2006; in final form February 2007)

In the present research study the primary aim is to understand and characterize the physical adsorption of polar molecules such as hydrogen cyanide (HCN) and methyl ethyl ketone (MEK), in silicalite-1, mordenite, and zeolite beta structures through detailed Monte-Carlo simulation studies. The sorption capacity and affinity of the different zeolites is compared by simulating single component isotherms for different Si/Al ratios at 298 K. It was found that the number of the Na^+ cations has an important effect on adsorption characteristics at lower pressures. In particular, within the range of [Na^+] studied, the adsorption capacity of these zeolites was found to be independent of the [Na^+], except in the case of zeolite beta. Furthermore, the MEK sorption capacity of zeolite beta was found to be the highest, followed by silicalite and mordenite respectively. The HCN sorption capacity of silicalite was shown to be greater than mordenite due to the presence of the 10-membered ring channels of silicalite.

Keywords: Hazardous molecules; Adsorption; Molecular modeling; Molecular simulation; Hydrogen cyanide; Methyl ethyl ketone

1. Introduction

Methyl ethyl ketone (MEK) is frequently used as a solvent for gums, resins, cellulose nitrate, as well as in consumer products such as lacquers, varnishes, paint removers, and glues [1,2]. Typically, it is released to air in gases emitted from the pertinent manufacturing industries producing the aforementioned products, or it is directly discharged in wastewater streams associated with a multitude of industrial processes. It is interesting to note that an exposure of 200 ppm of MEK causes irritation to the eyes, nose (mucous membranes) and throat. In addition to this, high MEK levels are associated with smog formation due to photochemical reactions with olefinic hydrocarbons [2,3]. In light of the above considerations and the hazardous nature of MEK under certain conditions, adsorption is considered to be one of the preferable and operationally advantageous methods to effectively remove MEK from industrial gases especially using activated carbon and zeolites as adsorbents [2].

Pursuing the above line of research, Yen *et al.* [2] carried out vapor phase adsorption experiments on zeolite Y and ZSM-5 for different Si/Al ratios varying from 5 to 31, where the concentration of MEK in the vapor phase was in the range of 100–1500 ppm. In this particular study, Zeolite Y was found to be more effective than ZSM-5 in removing MEK from the air stream under consideration. Furthermore, Monneyron *et al.* [4] conducted vapor phase single component and binary component (with toluene and 1,4-dioxane) adsorption experiments on zeolite Y and ZSM-5. They found that the component having the higher molecular weight adsorbed preferentially over the other, except in the case of MEK–toluene mixture adsorption on ZSM-5, where toluene sorption was less than MEK due to steric effects. Pires *et al.* [5] studied the effect of dealumination of zeolite Na–Y on the sorption of MEK at 298 K, and showed that an increase in the percentage of de-alumination reduced MEK adsorption, suggesting that sodium cations favor MEK. Uguina *et al.* [6] studied MEK desorption from silicalite and activated carbon beds, and suggested that the regeneration temperature for silicalite was in the range of 90–170°C, whereas in the case of activated carbon it was found to be within the range of 150–240°C. These findings suggest that dispersion interactions might be dominant in the case of silicalite, whereas electrostatic

*Corresponding author. Email: rwt@wpi.edu

Molecular Simulation
ISSN 0892-7022 print/ISSN 1029-0435 online © 2007 Taylor & Francis
http://www.tandf.co.uk/journals
DOI: 10.1080/08927020701275068

interactions might be dominant in the case of activated carbon due to the presence of acid sites.

Despite the aforementioned research efforts, the experimental data available in the pertinent body of literature are not currently adequate to understand the mechanism of MEK adsorption in activated carbons and zeolites, especially at the molecular level. Meininghaus *et al.* [7] obtained single component experimental data at relative pressure (P/P_{sat}) of 0.007 and showed that dealuminated zeolite Y has greater capacity than H-Mordenite and H—ZSM5 and Na—ZSM-5. Recently, Kotdawala *et al.* [8] studied the effect of sodium cations in zeolite Na—X, as well as hydroxyl, carbonyl and carboxylic sites in activated carbon on the adsorption capacity of MEK using molecular simulation methods, and suggested that the relative magnitudes of charge-dipole, dispersion, and charge-induced dipole interactions determine the sorption capacity of MEK in activated carbon and zeolite Na—X. In particular, it was suggested that MEK sorption capacity is less than 70 mg/g in zeolite—X as compared to activated carbon which displays a capacity ranging from 20–180 mg/g, depending on which functional sites exist in the carbon pore. However, to the best of our knowledge, the capacity and affinity of MEK sorption in silicalite, zeolite beta, and mordenite structures have not been yet adequately and systematically evaluated, either through experimental studies or simulation techniques. Indeed, these zeolites are likely to be good sorption candidates as their nominal pore sizes are slightly greater than the size of MEK molecules. Lack of experimental data and information of favorable sites in the aforementioned zeolites provide ample motivation and research incentive to study the adsorption of MEK using molecular simulation techniques.

In a conceptually similar methodological framework, the adsorption of hydrogen cyanide (HCN) was studied as well, recognizing that it is an acutely poisonous compound, which might enter the human body by breathing contaminated air. HCN vapors are commonly released into air from various sources, including vehicle exhaust emissions, chemical processing, extraction of gold and silver from low grade ores, metal plating, steel, iron, and finishing industries, petroleum refineries, and waste disposed in landfills. Currently, the best-known adsorbents for the removal of HCN from air are metal salt-impregnated activated carbons [9]. Freeman [9] and Reucroft [10] studied the adsorption of HCN and the mixture of HCN–water on BPL-activated carbon, a granular activated carbon supplied by Calgon Carbon Inc. The experimental results suggested that, adsorption of HCN strongly dominates over water, and HCN discourages additional adsorption of water vapor, which might be attributed to the greater polarizability and dipole moment of HCN.

In another study of the removal of HCN from air conducted by Oliver *et al.* [11], copper containing and copper-free activated carbons produced from porous sulfonated styrene/divinylbenzene resin were considered to assess the removal efficiency of HCN. The adsorbent performance was comparable to ASC Whetlerite carbons that contain salts of chromium, copper, and silver. Incorporation of copper into the starting material significantly increased HCN breakthrough times, but decreased the surface area and pore volume of the adsorbent. The results of X-ray photoelectron spectroscopy (XPS) analysis revealed partial or complete reduction of the starting divalent copper on the surface of the adsorbents, amply confirmed by the lack of formation of $(CN)_2$ during the adsorption of HCN, while the use of conventional Whetlerite carbon produced poisonous $(CN)_2$ gas. However, detailed and good-quality experimental data on the sorption of HCN from flue gases are limited, and do not suggest any suitable adsorbents for the removal of HCN. Recently, Kotdawala *et al.* [8] simulated the sorption characteristics of zeolite Na—X and activated carbon for HCN using molecular simulation methods, and suggested that Zeolite Na—X displays superior capacity than that of activated carbon due to the presence of cations which are responsible for large cation–dipole interactions. However, the pore size in the above simulations was of the order of 14–15 Å. Notice, that mordenite's 10-membered rings have openings of around 7 Å and its 12-membered rings have about 10 Å pores which might improve dispersion interactions with HCN molecules due to its high polarizability. Silicalite could in principle be a good candidate too, as it possesses 10-membered rings of approximately 5.6 Å diameter. Therefore, the smaller pore sizes of mordenite and silicalite, as well as the polarizability of HCN, suggested the study of the sorption of HCN, especially in the absence of enough and reliable experimental data [7].

The present paper is organized as follows: Section 2 provides a brief description of the particular atomistic modeling approach pursued, followed by a description of the molecular simulation methods employed in the context of the present study. Section 3 encompasses the paper's main results with a discussion about the primary findings. Finally, concluding remarks are provided in Section 4.

2. Molecular modeling and simulation framework

A pairwise-additive potential function is considered, which is comprised of a (12–6)-type of Lennard–Jones (LJ) potential term plus a purely Coulombic one, in order to quantitatively characterize the site–site non-bonded interactions [12]:

$$V_{ij} = 4\varepsilon_{ij}\left[\left(\frac{\sigma_{ij}}{r_{ij}}\right)^{12} - \left(\frac{\sigma_{ij}}{r_{ij}}\right)^{6}\right] + \frac{q_i q_j}{4\varepsilon_0 r_{ij}} \qquad (1)$$

where i and j are atoms of HCN/MEK or on the zeolite lattice, and r_{ij} is the distance between atoms i and j. ε_{ij} and σ_{ij} represent the LJ parameters, namely well-depth and diameter, respectively. Finally, q_i and q_j are the partial charges of the interacting sites.

The proposed modeling framework for the interacting sites is realized through the following three groups: HCN/MEK–HCN/MEK, Zeolite–Zeolite and Zeolite–HCN/MEK. The first two types of interacting sites (and the associated model parameters) were adequately characterized in the relevant literature from where we borrow the corresponding values [13–19], whereas the last one is assumed to obey the Lorentz–Berthelot mixing rules [20,21]:

$$\varepsilon_{ij} = \sqrt{\varepsilon_{ii}\varepsilon_{jj}} \quad \sigma_{ij} = \frac{\sigma_{ii} + \sigma_{jj}}{2} \tag{2}$$

MEK–MEK interactions were modeled using the Trappe-UA force field [13–16] in which the methyl sites were represented by a united atom, bonds were kept rigid, and angle bending and torsion terms were treated as flexible. The harmonic potential was used for angle bending and a cosine series form was used to account torsional interactions for sites separated by three bonds. The values of the parameters for angle bending and torsion interactions for MEK were taken from Stubbs *et al.* [16]. HCN–HCN interactions were modeled using the OPLS force field [17,18] in which bonds and angles are assumed rigid. The interaction parameters between the zeolite framework atoms and Na^+ cations in the framework were taken from Beerdsen *et al.* [19,20]

Table 1 contains all the pertinent zeolite, HCN and MEK interaction parameters. Furthermore, unit cell structures of silicalite, mordenite, and zeolite beta used in the present study are derived from studies conducted by Artioli *et al.* [22], Gramlich [23] and Newsam *et al.* [24], respectively. Finally, the justification for the particular procedure and basis for choosing Al sites in the mordenite and silicalite cases is thoroughly discussed in [20] and [25], respectively.

For Grand Canonical (μVT) Monte-Carlo simulations conducted in the context of the present research study, the Towhee [26] simulation package was used. Periodic boundary conditions were applied in all directions and an Ewald sum was explicitly used to calculate the electrostatic interactions [21]. For simulation purposes, two unit cells were considered in the silicalite case, four unit cells in mordenite, and four unit cells in the zeolite beta case. Final simulation box dimensions for silicalite were chosen as follows: $a = 20.0511$ Å, $b = 19.87570$ Å, $c = 26.73640$ Å, for mordenite $a = 18.011$ Å, $b = 20.53$ Å, $c = 30.112$ Å, and for zeolite beta $a = 25.32278$ Å, $b = 25.32278$ Å, $c = 26.40612$ Å. Cutoff distances for each simulation run were set less than half the shortest box side, in order to conform with the minimum image convention [21], namely 9.5 Å, 9.0 Å, and 12.0 Å for silicalite, mordenite and zeolite beta respectively. Simulation runs were initialized by considering Na^+ cations at their equilibrium positions. For this reason, NVT Monte-Carlo simulations were conducted, where the number of molecules, volume, and temperature were kept constant, and the Na^+ cations were placed near the aluminum sites. For each zeolite simulation box we placed 1–4 Na^+ cations per system (not per unit cell). These loadings correspond to Si/Al ratios of 197, 95, 63, and 47 for silicalite and mordenite, and 255, 127, 84, and 63 for zeolite beta. Then, for 10 million steps, Na^+ cations were displaced randomly and zeolite structures were kept fixed. Final positions of the Na^+ cations were fixed and used for future Monte-Carlo simulations in the (μVT) ensemble case.

Prior to these simulations, chemical potentials at each pressure point were computed by using the Widom Insertion Method [27] in a series of NPT Gibbs Ensemble Monte-Carlo (GEMC) simulation runs. [28,29] In this particular ensemble, pressure, temperature, and the number of fluid molecules were considered fixed. A simulation box containing 100 MEK (or HCN) molecules was set up. Translation and rotation moves of the MEK (or HCN) molecules and the volume change of the simulation box were sampled with probabilities of 50, 45 and 5%, respectively. At each pressure point the system was equilibrated for 20,000 cycles and a 20,000-cycle production run, followed by an equilibration run in which the chemical potential was calculated through the Widom Insertion Method every five cycles. Please notice, that a cycle corresponds to N Monte-Carlo moves, where N is the number of molecules in the system [20].

The chemical potentials calculated at each pressure point were used to set up the simulation runs in the grand canonical ensemble, and obtain the adsorption isotherms

Table 1. Zeolite, HCN and MEK interaction [13–19].

Lennard–Jones			*Coulombic*	
Interacting sites	*σ (A°)*	*ε (K)*	*Sites*	*q(e)*
O(MEK)	3.05	79.0	Si	2.050
C(MEK)	3.82	40.0	Al	1.75
CH_2 (MEK)	3.95	46.0	Na	1.0
CH_3(MEK)	3.75	98.0	[a]$OZ_{Si-OZ-Si}$/$OZ_{Si-OZ-Al}$	−1.025/−1.200
H(HCN)	0	0	O(MEK)	−0.424
N(HCN)	3.2	88	C(MEK)	0.424
C(HCN)	3.63	77	CH_3(MEK)	0
Si/Al	0	0	CH_2(MEK)	0
Na	2.33	46.8	H(HCN)	0.15
			C(HCN)	0.28
			N(HCN)	−0.43

[a]$OZ_{Si-OZ-Si}$: Oxygen of zeolite bridging two Si atoms, $OZ_{Si-OZ-Al}$: Oxygen of zeolite bridging Si and Al atoms.

of MEK (or HCN) in silicalite, mordenite, and beta zeolite structures. In these GCMC simulation runs insertion/deletion, regrowth, intramolecular atom translation, translation, and rotation of MEK (or HCN) molecules were sampled with probabilities of 30, 5, 5, 30 and 30%, respectively. No biasing was applied for insertions. Each simulation started with a 10 million step equilibration run, which was followed by a 10 million step production run. Statistical uncertainties were calculated by dividing the production run into ten blocks. Finally, the reader should be reminded that during the GCMC simulation runs both zeolite structures and cation positions were kept fixed [20,25].

3. Results and discussion

3.1 MEK sorption in silicalite, mordenite and zeolite beta

Figures 1 and 2 show the sorption capacity of zeolite beta with Si/Al ratios ranging from 63 to infinity. They suggest that the presence of Na^+ cations increases the sorption capacity (200 mg/g at Si/Al = 63 as compared to 50 mg/g for Si/Al → infinity) of zeolite beta by a factor of four, due to more pronounced electrostatic interactions. Also notice, that, an increase in the number of Na^+ ions in this framework does not seem to affect the capacity of zeolite beta at a higher operating pressure (4–5 kPa). However, figure 2 implies that the effect of Si/Al ratio remains significant in the low pressure regime. Figure 3 shows that MEK molecules are located in the short channels made of a 12 membered ring (7 Å). The polar part (white color) of MEK is pointed towards the sodium cations (blue), implying that electrostatic interactions may be influencing the sorption capacity of zeolite beta.

Sorption in silicalite and mordenite reveals that MEK has a high affinity for the silicalite pore surface and higher capacity than that of mordenite, as shown in figures 4 and 5. In particular, figure 4 shows that the sorption capacity of silicalite should be about 60% greater than that of mordenite. The presence of Na^+ ions improves the sorption capacity of mordenite slightly at low pressures, as seen in figure 5, but has less impact on its capacity at higher pressures (>1 kPa) as shown in figure 5. An increase in the number of cations in silicalite from 0 to 4 (from Si/Al = infinity to 47), increases sorption of MEK at low pressure significantly, as seen in figure 5, but the saturation capacity of silicalite decreases by 30% (figure 4). This can be explained by the presence of sodium cations which occupy some of the pore volume and lead to reduced capacity. The snapshots in figures 6 and 7 imply that sorption in silicalite might be reaching its saturation capacity as all molecules are in the straight/zig–zag channels located one by one in row without overlapping and utilizing all available pore volume (figure 6), but in the case of mordenite sorption reaches

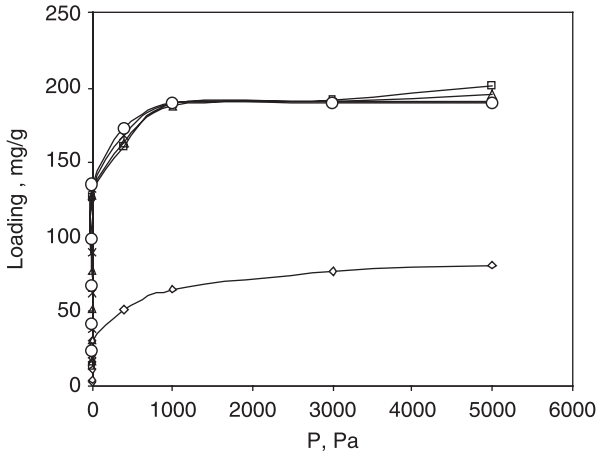

Figure 1. Sorption of MEK in Zeolite beta with different Si/Al ratios, Si/Al = 64 (○), 255 (□), 127 (Δ), Infinity (◇), 84 (*).

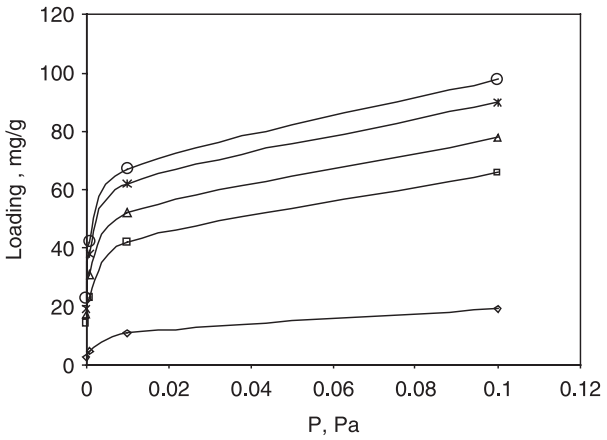

Figure 2. Sorption of MEK in Zeolite beta with different Si/Al ratios in the low pressure regime ratios Si/Al = 64 (○), 255 (□), 127 (Δ), Infinity (◇), 84 (*).

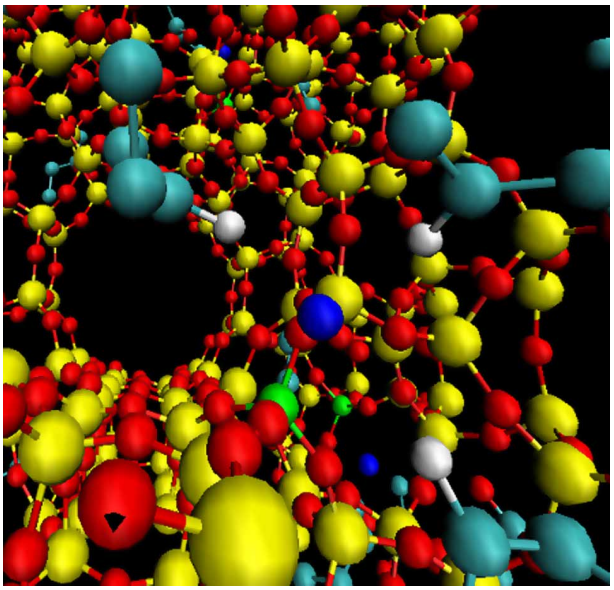

Figure 3. Prominent sites of MEK sorption in Zeolite beta with sodium cations.

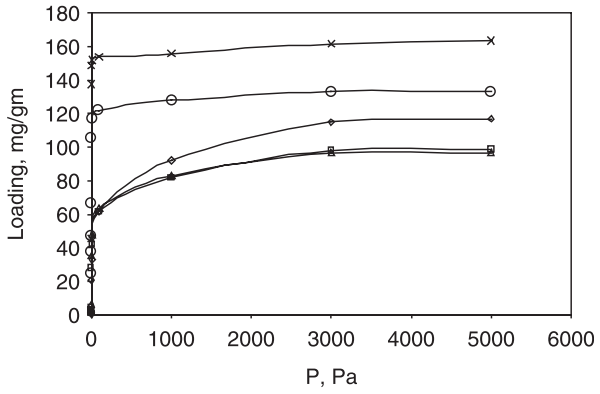

Figure 4. Sorption of MEK in silicalite and mordenite with different Si/Al ratios: for silicalite, Si/Al = 47 (○), infinity (*), and for mordenite, Si/Al = 197 (◇), 95 (□), 67 (Δ).

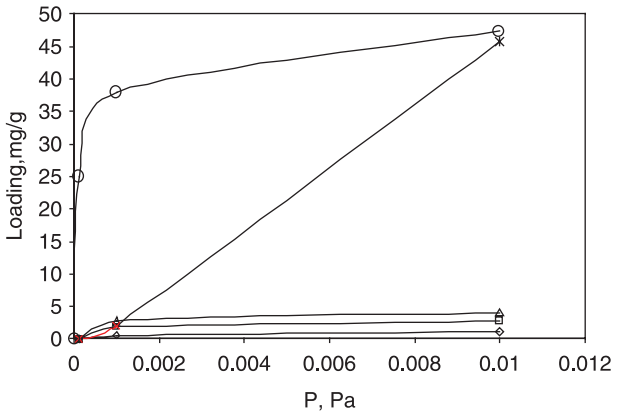

Figure 5. Sorption of MEK in silicalite and mordenite with different Si/Al ratios at low pressures: for silicalite, Si/Al = 47 (○), infinity (*), and for mordenite, Si/Al = 197 (◇), 95 (□ or □), 67 (Δ).

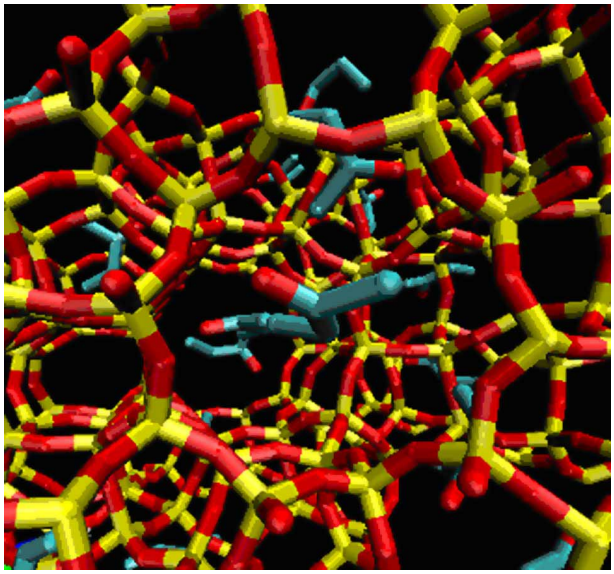

Figure 6. MEK sorption in straight channels of silicalite with Si/Al = infinity. (Silicon, yellow; oxygen, red; hydrogen, white; carbon/methyl/ethyl groups, cyan) (colour in online version).

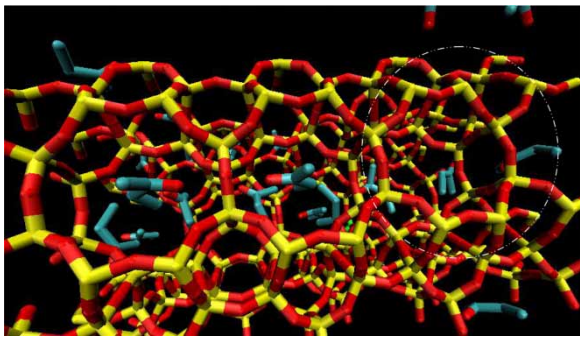

Figure 7. MEK molecules in 8 membered ring channels of mordenite with Si/Al = 95 (silicon, yellow; oxygen, red; hydrogen, white; carbon in methyl/ethyl groups, cyan) (colour in online version).

a plateau-like regime as some of the eight membered ring channels remain empty (see the white circle regime in figure 7).

Figure 8 shows sorption of MEK in mordenite with sodium cation. The "red" is an oxygen of carbonyl of the MEK and cyan color represents the nonpolar part of MEK consisting methyl and ethyl groups. Due to steric constraints the carbonyl of MEK is not pointed towards sodium cation (blue one) and hence the increase in sodium cations in mordenite does not improve the sorption capacity significantly (figure 5). However, in the case of silicalite, increasing the number of cations increases the sorption capacity at low pressure is illustrated in figure 9, where the carbonyl part of MEK (white) is pointed towards the sodium cation (blue) which increases the electrostatic interaction and hence the sorption.

3.2 HCN sorption in silicalite and mordenite

Sorption patterns in silicalite and mordenite reveal that HCN displays high affinity towards silicalite pore

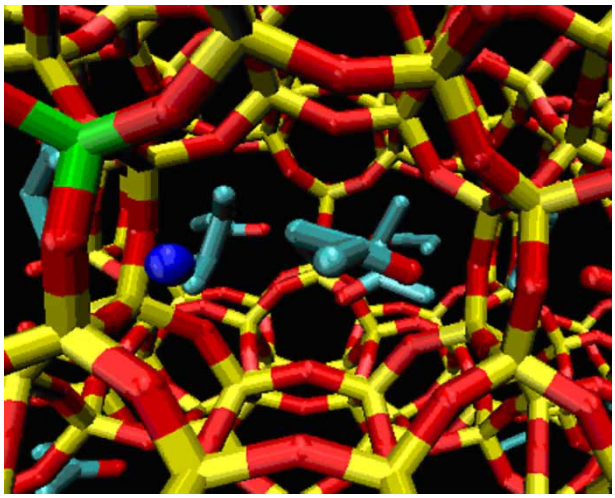

Figure 8. MEK molecules in 8-membered ring channels of mordenite with Si/Al = 95 (silicon, yellow; oxygen (in MEK carbonyl and silicalite), red, methyl/ethyl groups of MEK, cyan; and sodium, blue) (colour in online version).

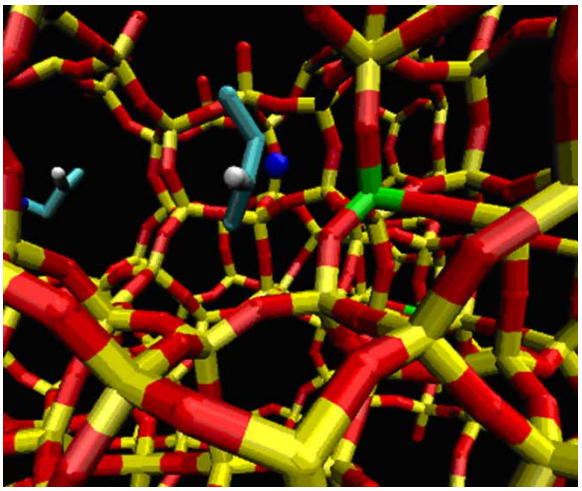

Figure 9. A typical configuration of MEK molecules in silicalite with Si/Al = 47, (sodium cation, blue; silicone, yellow; "O" of silicalite, red, methyl/ethyl groups of MEK, cyan; "O" of carbonyl of MEK, white; Al, green) (colour in online version).

surfaces, and a higher capacity (~150 mg/g) than that of mordenite (60–80 mg/g), as seen in figures 10 and 11. These differences may be attributed to the small channel size of the 10-membered rings of silicalite

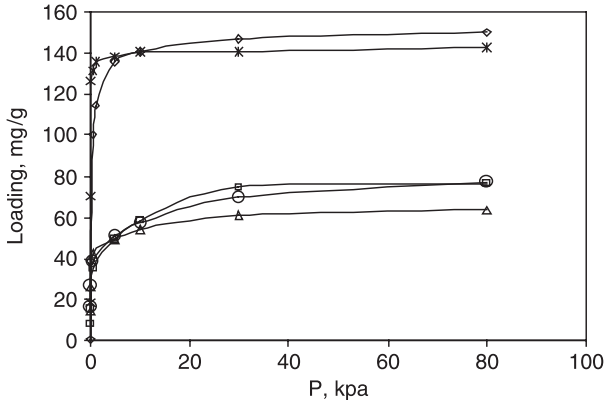

Figure 10. Sorption of HCN in silicalite and mordenite with different Si/Al ratios: for silicalite, Si/Al = 47 (*), infinity (◇), and for mordenite, Si/Al = 197 (□ or □), 95 (Δ), 63 (○).

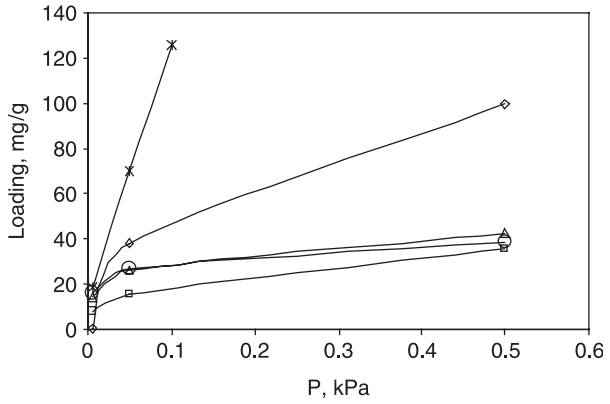

Figure 11. Sorption of HCN in silicalite and mordenite with different Si/Al ratios at low pressures: for silicalite, Si/Al = 47 (*), infinity(◇), and for mordenite, Si/Al = 197 (□), 95 (Δ), 63 (○).

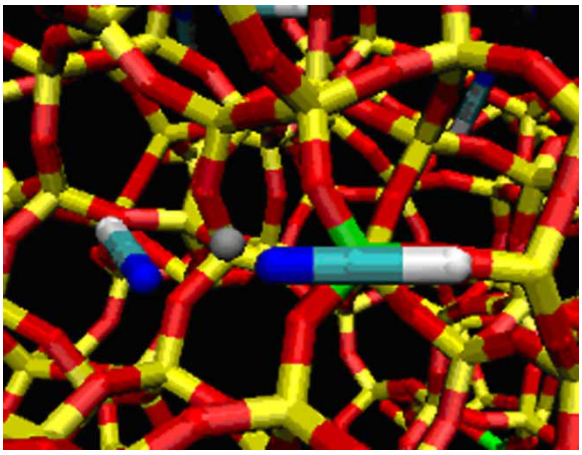

Figure 12. HCN molecules in silicalite with Si/Al = 47, (sodium cation, silver; "N", blue; silicone, yellow; "O", red; "C", cyan; "H", white) (colour in online version).

(approximately 5.6 Å) compared to mordenite's 12-membered channel which increases dispersion and electrostatic interactions. Figure 10 shows that the sorption capacity of silicalite was almost double than that of mordenites. The presence of Na^+ ions however, improves the sorption capacity of mordenites to some extent, as shown in figure 11, but has less influence on their saturation capacity. An increase in the number of cations in silicalite from 0 to 4 (i.e. Si/Al → infinity to 47) increases sorption of HCN at low pressure significantly, as seen in figure 11, but the saturation capacity of silicalite decreases slightly. Figure 12 shows the snap shot of HCN molecules in silicalite with sodium cations. The figure shows that negatively charged "N" of HCN (blue) is pointed toward the sodium cation (silver) suggesting that sodium cation improves sorption in silicalite and hence it increases the sorption capacity at lower pressure (figure 11). Figure 13 shows the hydrogen bonding among HCN molecules in silicalite in the straight and in the zig–zag channels (a train of molecules). However, the presence of sodium cations in

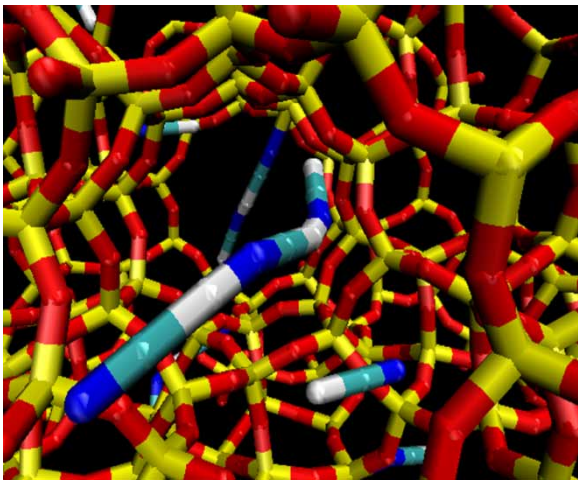

Figure 13. A "train" of HCN molecules in zig-zag channels of silicalite (N, blue; C, cyan; H, white) (colour in online version).

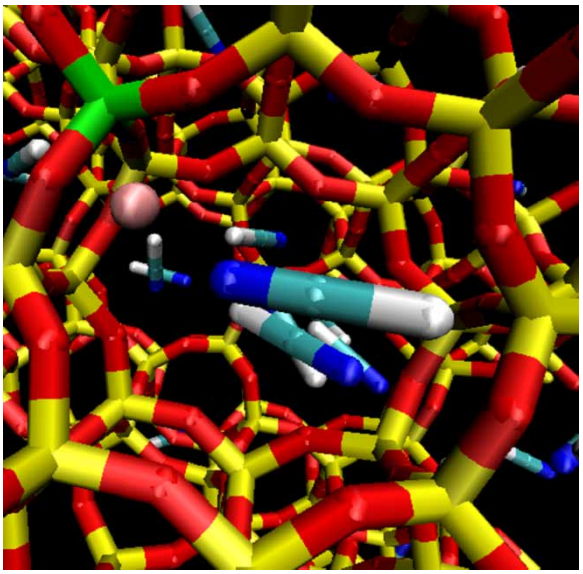

Figure 14. HCN molecule in the 8-membered ring channel of mordenite, "N" of HCN is pointed towards sodium cation (pink) which is near the Al atom (green) (colour in online version).

the intersection of straight and zig–zag channels disrupts the hydrogen bonding and reduces the sorption capacity of silicalite as seen in figures 12. Figure 14 shows a snapshot of HCN molecule adsorbed in 8-membered ring channel of mordenite with sodium cation. The figure implies that, due to the smaller size of the ring channel, HCN molecules cannot orient themselves to participate in hydrogen bonding with other HCN molecules. It also shows that the "N" of HCN (blue) is pointed towards sodium cation (pink).

The snapshot in figure 15 implies that HCN adsorption in silicalite without cations reaches a saturation capacity as most of the places in the silicalite appear to be occupied with HCN molecules at 80 kPa. However, the mordenite structure shows some unoccupied space at 80 kPa as seen in figure 16. This gives circumstantial evidence that in mordenite either the orientation of the molecules or the mordenite structure does not allow the utilization of the entire mordenite pore volume, or interactions with

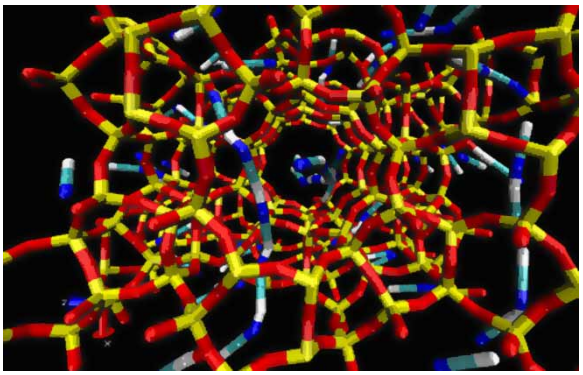

Figure 15. Pore filling by clustering of HCN in 10-membered straight and zig-zag channels of silicalite due to hydrogen bonding (silicon, yellow; oxygen, red; hydrogen, white; carbon, cyan; nitrogen, blue; sodium, green) (colour in online version).

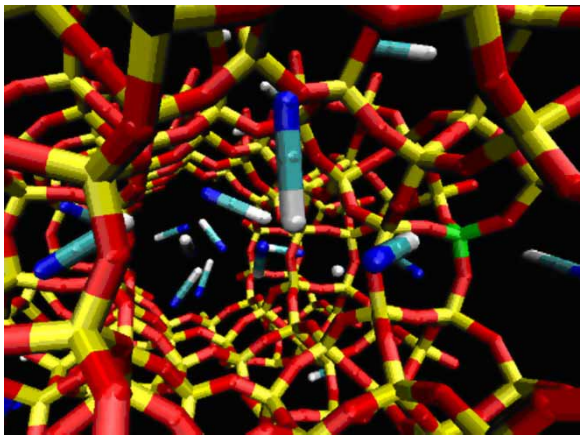

Figure 16. HCN sorption in the mordenite with Si/Al = 197 (silicon, yellow; oxygen, red, hydrogen, white; carbon, cyan, nitrogen, blue; sodium, green) (colour in online version).

mordenite and other HCN molecules are not enough to fill mordenite structure with HCN.

4. Conclusions

Monte-Carlo simulations for HCN and MEK adsorption studies in silicalite, mordenite and zeolite beta structures with different Na^+ cation loadings were carried out. The results reveal the importance of the pore structure and cation concentration on the adsorption of MEK and HCN. Although these three zeolites have similar pore volumes, zeolite beta, with its pore structure being mostly accessible to MEK molecules, is predicted to adsorb significantly more MEK than silicalite and mordenite. The greater affinity of silicalite towards HCN and MEK as compared to mordenite was attributed to its pore size of 5.6 Å that directly contributes to the underlying Van der Waals and electrostatic interactions. Furthermore, the presence of sodium cations increases the sorption capacity of zeolite beta, mordenite and silicalite at relatively low pressures, but does not influence the capacity at higher pressures of the zeolite under consideration. It was also found, that the sorption of MEK/HCN in silicalite occurs only in the 10-membered ring channels (both zig–zag and straight), due to its size which is comparable to the channel size. In addition, the sorption of MEK in mordenite was mainly observed in the 8 and 12-membered ring channels. The intersection of 8- and 12-membered ring channels was identified as the most active sites for sorption due to the presence of cations. Finally, in the case of zeolite beta, 12-membered ring long and short channel intersections were shown to be quite important for MEK sorption as all sodium cations are placed at the intersection.

Acknowledgements

The authors gratefully acknowledge the support provided by the National Science Foundation (NSF) through grant: NSF

NIRT award DMI-0210258. This work was also supported by the following NSF programs: Partnerships for Advanced Computational Infrastructure, Distributed Terascale Facility (DTF), and Terascale Extensions: Enhancements to the Extensible Terascale Facility. Technical help on computing platforms from Josh Brandt, WPI Computing and Communications Center, Senior UNIX Systems Administrator, is gratefully acknowledged as well.

References

[1] http://www.spacelab.com/compound/c78933.htm
[2] S.H. Yen, F.T. Jeng, J.H. Tsai. Adsorption of methyl ethyl ketone vapors on to zeolites. *J. Environ. Sci. Health A*, **32**(8), 2087 (1997).
[3] S.W. Blocki. Hydrophobic zeolite adsorbent: a proven advancement in solvent separation technology. *Environ. Prog.*, **12**, 226 (1993).
[4] P. Monneyron, M. Manero, J. Foussard. Measurement and modeling of single- and multicomponent adsorption equilibria of VOC on high-silica zeolites. *Environ. Sci. Technol.*, **37**, 2410 (2003).
[5] J. Pires, A. Carvalho, P. Veloso, M.B.D. Carvalho. Preparation of dealuminated faujasites for adsorption of volatile organic compounds. *J. Mater. Chem.*, **10**, 3100 (2002).
[6] M.A. Uguina, J.L. Sotelo, J.A. Delgado, J.M. Gomez, L.I. Celemin. Adsorption of methyl ethyl ketone and trichloroethylene from aqueous solutions on the silicalite fixed bed adsorbers. *Sep. Purif. Technol.*, **42**, 91 (2005).
[7] C.K.W. Meininghaus, R. Prins. Sorption of volatile organic compounds on hydrophobic zeolites. *Microporous Mesoporous Mater.*, **35–36**, 349 (2000).
[8] R.R. Kotdawala, N. Kazantzis, R.W. Thompson. Molecular simulation studies of adsorption of hazardous molecules in zeolite—X and activated carbons: the hydrogen cyanide and methyl ethyl ketone cases. *J. Hazard. Mater.*, (under review).
[9] G.B. Freeman, P.J. Reucroft. Adsorption of HCN and H_2O vapor mixtures by activated and impregnated carbons. *Carbon*, **17**, 313 (1979).
[10] P.J. Reucroft, P.B. Rao, G.B. Freeman. Binary vapor adsorption by activated carbon. *Carbon*, **21**, 171 (1983).
[11] T.M. Oliver, K. Jugoslav, P. Aleksandar, D. Nikola. Synthetic activated carbons for the removal of hydrogen cyanide from air. *Chem. Eng. Process.*, **44**, 1187 (2005).
[12] C.E. Ramachandran, S. Chempath, L.J. Broadbelt, R.Q. Snurr. Water adsorption in hydrophobic nanopores: Monte Carlo simulations of water in silicalite. *Microporous Mesoporous Mater.*, **90**, 293 (2006).
[13] M.G. Martin, J.I. Siepmann. Transferable potentials for phase equilibria. 1. United-atom description of *n*-alkanes. *J. Phys. Chem. B*, **102**, 2569 (1998).
[14] M.G. Martin, J.I. Siepmann. Novel configurational-bias Monte Carlo method for branched molecules. Transferable potentials for phase equilibria. 2. United-atom description of branched alkanes. *J. Phys. Chem. B*, **103**, 4508 (1999).
[15] B. Chen, J.J. Potoff, J.I. Siepmann. Monte Carlo calculations for alcohols and their mixtures with alkanes. Transferable potentials for phase equilibria. 5. United-atom description of primary, secondary and tertiary alcohols. *J. Phys. Chem. B*, **105**, 3093 (2001).
[16] J.M. Stubbs, J.J. Potoff, J.I. Siepmann. Transferable potentials for phase equilibria. 6. United-atom description for ethers, glycols, ketones and aldehydes. *J. Phys. Chem. B*, **108**, 17596 (2004).
[17] W.L. Jorgenson, J.M. Briggs. Monte Carlo simulations of liquid acetonitrile with a three-site model. *Mol. Phys.*, **63**, 547 (1988).
[18] W.L. Jorgenson, D.S. Maxwell, J. Tirado-Rives. Development and testing of the OPLS all-atom force field on conformational energetics and properties of organic liquids. *J. Am. Chem. Soc.*, **118**, 11225 (1996).
[19] E. Beerdsen, D. Dubbledum, B. Smit, T.J.H. Vlugt, S. Calero. Simulating the effect of Non-framework cations on the adsorption of alkanes in MFI-type zeolites. *J. Phys. Chem. B*, **107**, 12088 (2003).
[20] A.O. Yazaydin, R.W. Thompson. Molecular simulation of adsorption of MTBE in silicalite, mordenite, and zeolite beta. *J. Phys. Chem. B*, **110**, 14458 (2006).
[21] M.P. Allen, D.J. Tildesley. *Computer Simulation of Liquids*, Clarendon Press, Oxford (1989).
[22] G. Artioli, C. Lamberti, G.L. Marra. Neutron powder diffraction study of orthorhombic and monoclinic defective silicalite. *Acta Crystallogr. B*, **56**, 2 (2000).
[23] V. Gramlich, Ph.D. Thesis, ETH, Zürich, Switzerland (1971).
[24] J.M. Newsam, M.M.J. Treacy, W.T. Koetsier, C.B. de Gruyter. Structural characterization of zeolite beta. *Proc. R. Soc. Lond. A Math. Phys. Eng. Sci.*, **420**, 375 (1998).
[25] A.O. Yazaydin, R.W. Thompson. Simulating the vapour–liquid equilibria of 1,4-dioxane. *Mol. Simul.*, **32**, 657 (2006).
[26] http://towhee.sourceforge.net
[27] B. Widom. Some topics in the theory of fluids. *J. Chem. Phys.*, **39**, 2802 (1963).
[28] A.Z. Panagiotopoulos. Direct determination of phase coexistence properties of fluids by Monte Carlo simulation in a new ensemble. *Mol. Phys.*, **61**, 813 (1987).
[29] A.Z. Panagiotopoulos, N. Quirke, M. Stapleton, D.J. Tildesley. Phase equilibria by simulation in the Gibbs ensemble. Alternative derivation, generalization, and application to mixture and membrane equilibria. *Mol. Phys.*, **63**, 527 (1988).